Jun 28th, 4:00 PM

Cross-Section Influence on Velocity Distribution & Energy Dissipation of a Moderately Sloped Spillway Chute Flow

A. Tohidi
Clemson University, atohidi@g.clemson.edu

Farzam Safarzadeh Maleki
Massachusetts Maritime Academy, fmaleki@maritime.edu

Recommended Citation

Tohidi, A., Safarzadeh Maleki, F. (2016). Cross-Section Influence on Velocity Distribution & Energy Dissipation of a Moderately Sloped Spillway Chute Flow. In B. Crookston & B. Tullis (Eds.), Hydraulic Structures and Water System Management. 6th IAHR International Symposium on Hydraulic Structures, Portland, OR, 27-30 June (pp. 457-466). doi:10.15142/T3460628160853 (ISBN 978-1-884575-75-4).

6th International Symposium on Hydraulic Structures Portland, Oregon, USA, 27-30 June 2016
Hydraulic Structures and Water System Management
ISBN 978-1-884575-75-4 DOI: 10.15142/T3460628160853

Cross-Section Influence on Velocity Distribution & Energy Dissipation of a Moderately Sloped Spillway Chute Flow

A.Tohidi[1], and F. S. Maleki[2]
[1]Glenn Dept. of Civil Engineering,
Clemson University,
Clemson, SC, 29634,
USA

[2]Assistant Professor of Engineering
Massachusetts Maritime Academy,
Buzzards Bay, MA, 02532,
USA
E-mail: fmaleki@maritime.edu

ABSTRACT

Erosion at the dam toe due to potential to kinetic energy conversion of the outlet release is a complex yet fascinating engineering challenge. The energy dissipation due to flow separation at sharp cornered geometries affects the flow stream and causes the lower velocity at the dam's toe. To date, many of the conventional dam engineering techniques consider the dam toe as the examination point. In this research, by the use of OpenFOAM numerical model, the water flow in the spillway chute is modeled. The velocity profile of the chute flow in three different cross-sections is considered for the same outlet boundary conditions. The effect of geometry on kinetic energy (velocity) reduction has been studied in order to find a trend for this type of energy cascade. Simulation results show that lateral eddies form due to generation of translatory waves and aeration processes in trapezoidal and curved edge rectangular cross sections. While these type of cross sections might be of use from the energy dissipation perspective, the higher velocities may deliver higher stagnation or uplift pressures in cases of vertical offset on the spillway's slab (bed).

Keywords: Erosion, Energy Dissipation, Spillway Chute, OpenFOAM, Numerical Modeling.

1. INTRODUCTION

Dams play a significant role in efficient control of a flood from extreme hydrological events. A rise in the reservoir's water level will be induced by the substantial inflow during intense rainfalls. Hence, spillways are designed to convey the excess water in a controlled and non-destructive fashion. On this matter, a key aspect of spillway design is energy dissipation. The energy dissipation system in most of the dams consists of a spillway crest, a water conveying part, and a terminal structure at the downstream. A poor design in any part of the spillway may cause dam failure (Christodoulou 1993; Lempérière et al. 2012; Chanson 2015).

The enormous energy release of large inflows over spillways necessitates a design such that energy cascades without considerable damage to the hydraulic structures, facilities downstream, and surrounding environment. This process is strongly dependent on the geometry and design of the water conveying part of the dissipater system. With regard to this, the water conveying part of spillways should be designed in order to deliver a stable free surface flow and lower the risk of localized failure due to defects and anomalies on the bed surface. One of the common designs, especially in concrete gravity dams, is chute spillways as they are usually not intended to dissipate energy like stepped spillways (Tanchev 2014). Design characteristics of this type of spillways are very well documented; see for example (Ippen and others 1951; Reinauer and Hager 1998). Yet, the main objective of this study is to investigate the effects of cross section geometry on the energy dissipation behavior of the smooth (without baffle blocks) chute spillways. Although there has been some studies on the effects of geometry on the free surface flow through chute spillways (Ellis and Pender 1982; Montes 1994; Song and Zhou 1999), the influence of various cross section geometries on the energy dissipation behavior is less considered. This could be an arduous task with costly testing

prototypes. However, with recent advancements both in computational fluid dynamics (CFD) algorithms and high performance scientific computing, it is now possible to model a full-scale chute spillway with different geometries in 3D and observe the effects.

In the present study, three cross sections, i.e. rectangular, trapezoidal, and rectangular with curved edges, are examined numerically by simulating multiphase (air-water) flow through chute spillways. The main motive behind adopting the initial conditions and geometric parameters is the failure of Big Sandy Dam's spillway due to pressure stagnation (Billington et al. 2005). This document particularly deals with simulation of the transport processes through the aforementioned cross sections and studies the distribution of velocity, water phase fraction, and pressure across the depth of the downstream end of the spillway. Since the final design depends on many different parameters, this study just presents the exploratory results, which are not conclusive for engineering practice. Section two presents the adopted numerical model and solution procedure. Section three presents the results and relevant discussions, and, finally, section four delivers the concluding remarks.

2. NUMERICAL MODEL

Supercritical flow in the chute spillway along with certain geometric characteristics of the cross section may lead to cavitation, shock (interface) waves, translatory waves, and aeration of the flow (Abbasoglu and Okay 1992; Kökpinar and Göugücs 2002; Novák et al. 2007; Tanchev 2014). In order to capture the essential physics behind these phenomena, the turbulent flow and flow separation processes should be taken into account. This is done by solving Reynolds Averaged Navier-Stokes (RANS) equations for a case that serves as a close approximation to the chute spillway of Big Sandy Dam with three different cross section configurations (see section 3) by utilizing an open source computational fluid dynamics C++ library called OpenFOAM (Jasak et al. 2007). The following subsections present the governing equations, numerical solution method, and simulation parameters, respectively.

2.1. Governing Equations & Computational Domain

Navier-Stokes equations are fundamental governing equations of the fluid motion given the fluid is a continuum medium. The governing partial differential equations, for incompressible isothermal fluids at relatively low Mach numbers (less than one), are conservation of momentum and conservation of mass. They, respectively, read as

$$\rho \frac{D\boldsymbol{U}}{Dt} = -\nabla p + \mu \nabla^2 \boldsymbol{U} + \rho \boldsymbol{g} \tag{1}$$

$$\nabla \cdot \boldsymbol{U} = 0 \tag{2}$$

where D is material derivative, $\boldsymbol{U}$ is instantaneous velocity vector, p is pressure, μ is dynamic viscosity, and ρ is the fluid's density. Also, $\boldsymbol{g}$ is the gravity acceleration vector. Through this study, instead of modeling the actual slope of the steeped chute spillway, the complete geometry is considered in the Cartesian coordinates where the gravity acceleration vector is decomposed in three dimensions as $(gsin(\theta), 0, -gcos(\theta))$; Figure 1 shows schematic view of the computational domain and geometric outline of the cross sections. For complete derivation of the governing equations, see Kundu et al. (2002).

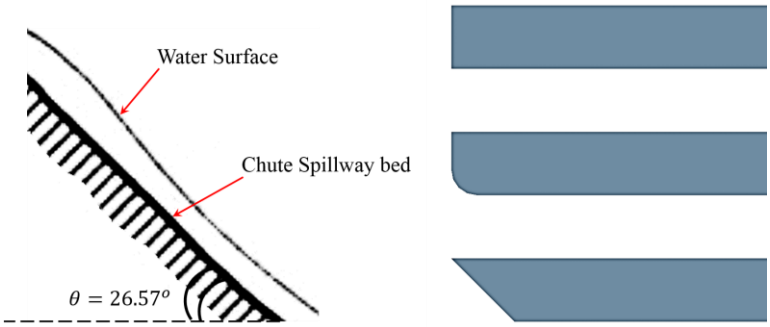

Figure 1. (Left) Side view schematic of the chute spillway and (Right) outline of cross sections from front view.

2.2. Numerical Solution Method

The solution domain is discretized into a finite number of small control volumes, mostly hexahedron shapes, and the governing equations are averaged over each control volume. For details of this method, that is finite volume method (FVM), see (Ferziger and Peric 2012). The feature of the flow in the chute spillways is the unsteady transport of air and water by a recognizable interface. This is resolved using volume of fluid (VOF) method in which a specie transport equation is used to determine the relative volume fraction of the air and water (Hirt and Nichols 1981). The volume fraction of water to the control volume is shown by α throughout this work. The phase fraction can be any value between 0 and 1 (totally water), and the solver (interFoam) uses a multi-dimensional universal limiter for explicit solution (MULES) method to maintain boundedness of each phase fraction independent of the time marching schemes. The convection terms in momentum equations are discretized using the Gauss Linear Upwind method. Also, the phase fraction convection term is resolved by Gauss Van Leer scheme to ensure stability. For the rest of the terms in governing equations, Gauss Linear Corrected scheme is adopted. Going to the details of the solver, particularly time marching algorithms, in not within the scope of this study. Therefore, see the OpenFOAM programmer's guide for a thorough explanation.

2.3. Turbulent Flow Model

According to the Bureau of Reclamation's report, the chute spillway at Big Sandy Dam failed due to uplift stagnation pressure at failure velocity of $U=9.45\ {}^{m}/_{s}$. This leads to the fact that Reynolds' number of the flow is of the order of $O(10^6 - 10^7)$ in this case. Hence, the flow is fully turbulent, and velocity and pressure fluctuations need to be taken into account.

Both Direct Numerical Simulations (DNS) and Large Eddy Simulations (LES) give a fine time-varying turbulent velocity field (Pope 2000). However, their computational cost is significantly higher than RANS methods. For engineering purposes in which the range of 5% error is acceptable and high resolution of the flow is not needed, RANS models work perfectly for describing the flow behavior. Several surveys such as that conducted by Bombardelli et al. (2011) & Valero and Bung (2015) provide more information on applications, capabilities, and limitations of RANS models in simulating spillway flows. In RANS methodology, time-averaging of governing equations introduces a nonlinear term called Reynolds' stress term into momentum equations (Pope 2000). In order to model this term, manifold RANS closures models are proposed (Pope 2000). Here, the well-known standard κ-ε model is employed since the flow is fully turbulent and effects of molecular viscosity are negligible. Basically, in addition to the time-averaged governing equation, two more equations for turbulent kinetic energy ($k = 1/2\ \overline{u_i' u_i'}$) and dissipation rate of kinetic energy (ε) should be solved. Overbar notation denotes the time-averaged quantities of each term. The equations for turbulent kinetic energy and dissipation rate are as follows if overbar notation is ignored for simplicity.

$$\frac{\partial k}{\partial t} + U_j \frac{\partial k}{\partial x_j} = \frac{\partial}{\partial x_j}\left[\left(\nu + {}^{\nu_t}/_{\sigma_k}\right)\frac{\partial k}{\partial x_j}\right] + \tau_{ij}\frac{\partial U_i}{\partial x_j} - \varepsilon \tag{3}$$

$$\frac{\partial \varepsilon}{\partial t} + U_j \frac{\partial \varepsilon}{\partial x_j} = \frac{\partial}{\partial x_j}\left[\left(\nu + {\nu_t}/{\sigma_\varepsilon}\right)\frac{\partial \varepsilon}{\partial x_j}\right] + C_{\varepsilon 1}\frac{\varepsilon}{k}\tau_{ij}\frac{\partial U_i}{\partial x_j} - C_{\varepsilon 2} \quad (4)$$

$$\nu_t = C_\mu {k^2}/{\varepsilon} \quad (5)$$

$$C_{\varepsilon 1} = 1.44,\ C_{\varepsilon 2} = 1.92,\ C_\mu = 0.09,\ \sigma_k = 1.0,\ \sigma_\varepsilon = 1.3 \quad (6)$$

where U is now the time-averaged velocity, ν is kinematic viscosity, and ν_t is the eddy viscosity. Also, subscripts i, j represent the coordinate system directions in Einstein notation. In addition, τ_{ij} is the Reynolds' shear stress tensor. Details of the κ-ε model in multiphase flow simulations are very well documented (Jones and Launder 1972). In this work, standard coefficients of the κ-ε model, as shown above, are used. Performance validation of κ-ε model and two-phase flow solvers of OpenFOAM are beyond the scope of this study although the failure depth and velocity of the Big Sandy Dam is obtained within a narrow error margin; see section 3. However, for supplementary details on validation of OpenFOAM solvers over various length and time scales, see Deshpande et al. (2012) and Lopes (2013).

2.4. Simulation Parameters

As mentioned before, the goal of this study is to investigate the energy dissipation behavior with change in cross section geometry while the failure conditions of Big Sandy Dam's spillway are reached. Based on the available characteristics of the Big Sandy Dam (Reclamation Magazine 2012), the failure discharge is 11.33 ${m^3}/{s}$, with uniform failure velocity of 9.45 ${m}/{s}$ in a rectangular cross section. Therefore, the failure initial depth for the flow inside the chute spillway is 0.09-m. The slope of the spillway, i.e. θ, is considered to be 26.57° with horizon, which is a relatively moderate slope for chute spillways. Specifics of the chute spillway's simulation models are presented in Table 1.

On this matter, the minimum mesh size is found through a mesh convergence analysis that will be presented in next section. Implemented boundary conditions on the computational domain are also shown in Figure 2.

Table 1. Specifics of the chute spillway simulation models.

Cross section	Dimensions (m)	Minimum mesh size (m) – Mesh type
Rectangular	20 × 13.32 × 0.5	0.1 × 0.1 × 0.05 – structured Hexahedron
Rectangular with curved side edges at bed	20 × 13.32 × 0.5*	0.1 × 0.1 × 0.05 – unstructured Hexahedron
Trapezoidal	20 × 12.32 with 45° slope up to 13.32 at the top × 0.5	0.1 × 0.1 × 0.05 – unstructured Hexahedron

* Curved edges have 0.2-m radius

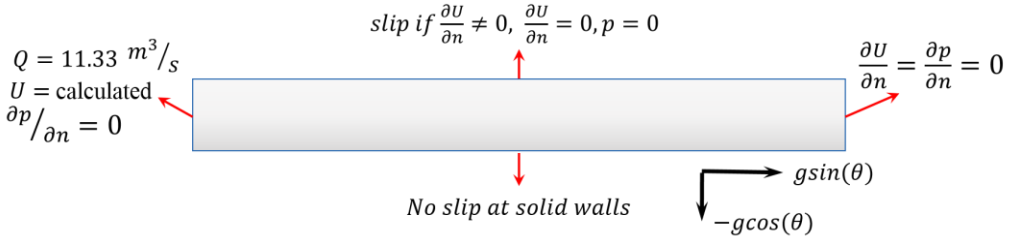

Figure 2. Schematic, side view (X-Z plane), diagram of implemented boundary conditions for pressure and velocity at the inlet in left, solid walls at the bottom and sides of the domain, atmosphere on top, and outlet at right.

As for of the turbulence model initial conditions at the inlet, the flow height is chosen such that it satisfies two conditions. Firstly, the inflow remains constant and equal to the critical failure discharge of Big Sandy Dam, at least in the rectangular section. Secondly, the hydraulic radius of the cross sections remains in the same order. Turbulent mixing length is considered to be 7% of the hydraulic radius of the cross sections. Additional inlet details are given in Table 2, assuming that the turbulence intensity for all cases is 5%.

Table 2. Inlet values of the turbulence model.

Turbulence parameters	Rectangular	Rectangular with curved edges	Trapezoidal
$l = 0.07R_h$	0.0630	0.0600	0.1310
$k = 1.5(UI)^2$	0.0920	0.0110	0.0170
$\varepsilon = C_\mu k^{1.5}/_l$	0.0399	0.0017	0.0009
$\nu_t = C_\mu k^2/_\varepsilon$	0.0191	0.0660	0.0142

The simulations are conducted with 380 Intel Xeon E5-2665 cores on Clemson University's Palmetto cluster. The initial time step is chosen such that the Courant Number in each case is less than 1, i.e. $\delta t = 0.001\ (s)$. However, OpenFOAM's interFom solver has this ability to adapt the time step with the maximum allowable Courant number, which is introduced to be 0.7 in all simulations.

3. RESULTS & DISCUSSIONS

The first set of analysis examined the convergence of solutions by decreasing the mesh size in Z direction. Figure 3, illustrates the velocity profiles through water and air depth with increments of 0.1, 0.08, and 0.05 m. Considering symmetry of the flow, the profiles are extracted from the centerline of the rectangular cross section at the outlet. The difference between 0.08-m and 0.05-m mesh size is less than 5% and is in the acceptable range for engineering applications. Therefore, for the rest of simulations $dz = 0.05\ m$ is adopted.

Energy dissipation behavior including processes like cavitation, interface waves, translator waves, and aeration can be understood from the quasi-steady state of the water surface through the domain. Thus, the kinetic energy of the simulations is recorded through the simulations to determine when the average flow is relatively steady. Figure 4, demonstrates time history of the turbulent kinetic energy during 15 seconds of the simulations at a point with coordinates of (15, 6.66, 0.01) meters through the water phase.

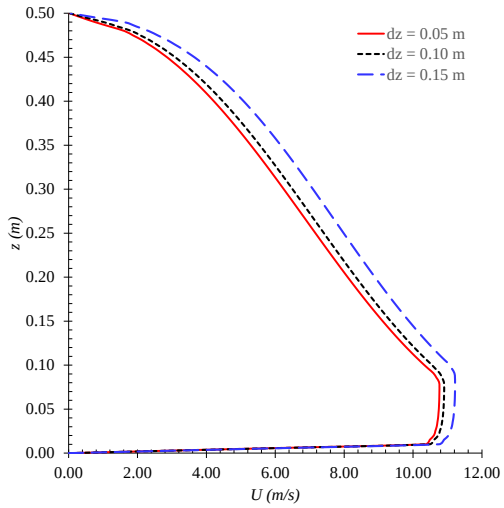

Figure 3. Mesh convergence analysis based on the velocity distribution over two phases, i.e. water and air in rectangular cross section. The velocity profiles are extracted from the centerline of the domain at the outlet.

Since it is shown that after 15 seconds the chute spillway flow is quasi-steady, discussions will be based on the results at 15 seconds. In order to validate the simulation outputs, results of the rectangular cross section are compared with the failure state of the Big Sandy Dam's chute spillway (Billington et al. 2005; Reclamation Magazine 2012). The simulation results extracted at 10 m downstream from the inlet. Results show a fully turbulent velocity profile with maximum value of 9.11 $^{m}/_{s}$, which delivers only 3.7% error compared to the reported failure velocity in the Big Sandy Dam case; see Figure 5. Note that markers in all figures are for visualization purposes and don't correspond to the face or cell-center values of the mesh in simulations. Also, Figure 5 shows phase fraction distribution of water through the depth, and, as can be seen, the failure depth of water is captured almost exactly equal to 0.09 m.

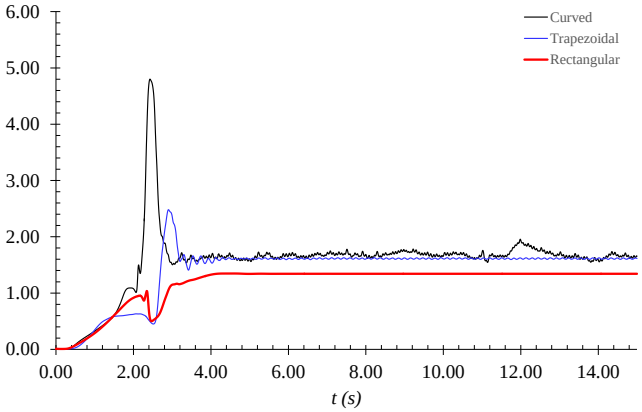

Figure 4. Time history of the turbulent kinetic energy at a point with coordinates of (15, 6.66, 0.01) meters through the water phase.

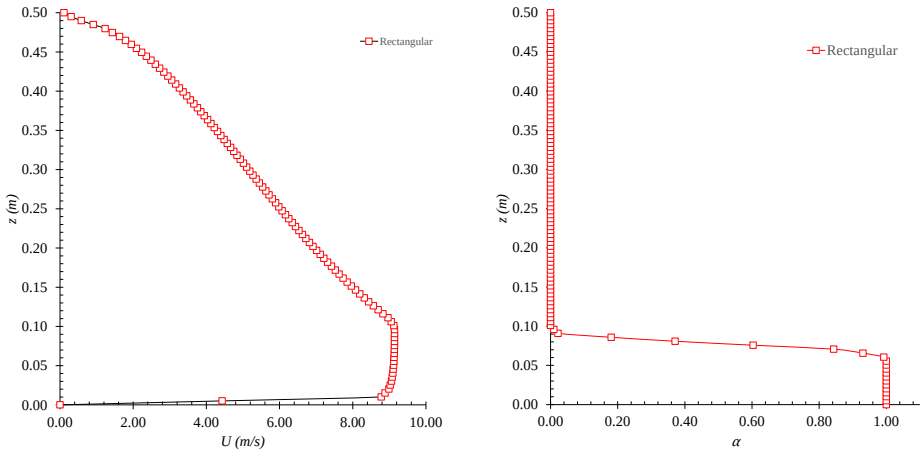

Figure 5. (Left) Vertical velocity profile of the chute spillway with rectangular cross section at the center-line of the cross section in 10-m downstream. (Right) Corresponding water phase fraction distribution through the depth of the flow.

Figure 6 shows the contour plots of the water surface corresponding to phase volume fraction of water, $\alpha = 0.99$. The α is chosen only for visualization purposes to provide a smooth surface translator waves. Considering the energy dissipation of the flow through different cross sections by lateral eddies, three observations can be noted. First, formation of a stationary interface wave (not shown here) due to considerable inflow inside the chute spillway domain. Since this type of wave is immediately convected downstream of the spillway, it doesn't interfere with the energy dissipation process (Tanchev 2014). Second, generation of translatory waves that move along the flow towards the terminal structure. These waves are observed mainly in curved edge rectangular and trapezoidal cross sections and cause non-stationary impulses into the main dissipator structure at downstream end. As shown in Figure 6, translatory waves are propagated through the entire width of the curved edge rectangular cross section whereas in the trapezoidal cross section, they are localized on the sides. Although these waves may dissipate energy early and well before the main dissipator structure, they may cause overflowing of water. The third observation is the aeration, which contributes to the energy dissipation (Tanchev 2014). Aeration develops where turbulent boundary layer starts to penetrate the full depth of the flow in spillway (Tanchev 2014). The approximate aeration length can be calculated using Hickot's equation (Novák et al. 2007), $14.7q^{0.53}$, where q is the unit discharge per width. The aeration length for the trapezoidal and curved edge rectangular cross sections, with 0.795 and 0.854 m^2/s unit discharge, is 13.05-m and 13.54-m downstream, respectively. This shows that the aeration point and location of non-stationary impulses of translatory waves occur adjacent to each other. Therefore, the energy dissipation due to aeration and energy loss on the water surface starts earlier inside the chute spillway channel for trapezoidal and curved edge rectangular cross sections compared to rectangular cross sections.

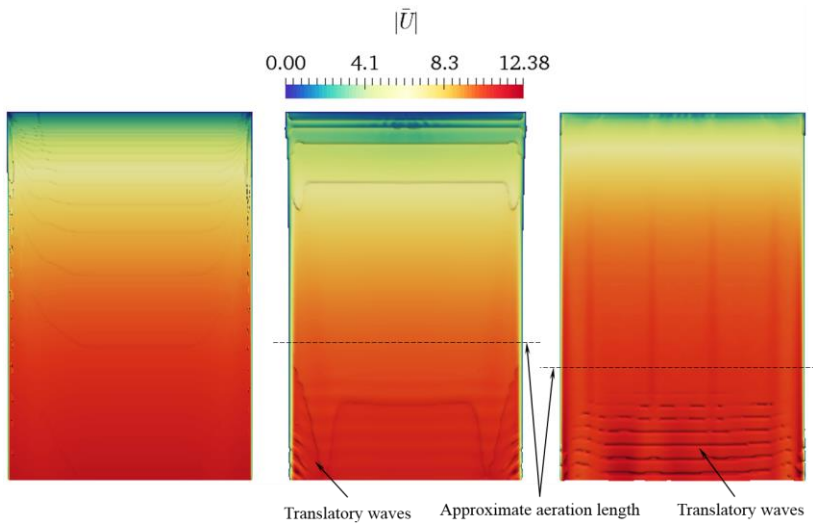

Figure 6. Contour plots of water surface with phase volume fraction of $\alpha = 0.99$ overlaid with contours of time-averaged velocity magnitude. On the left is rectangular section, in the middle is the chute spillway with trapezoidal cross section, and at the right is the spillway with rectangular yet curved edges at bottom cross section.

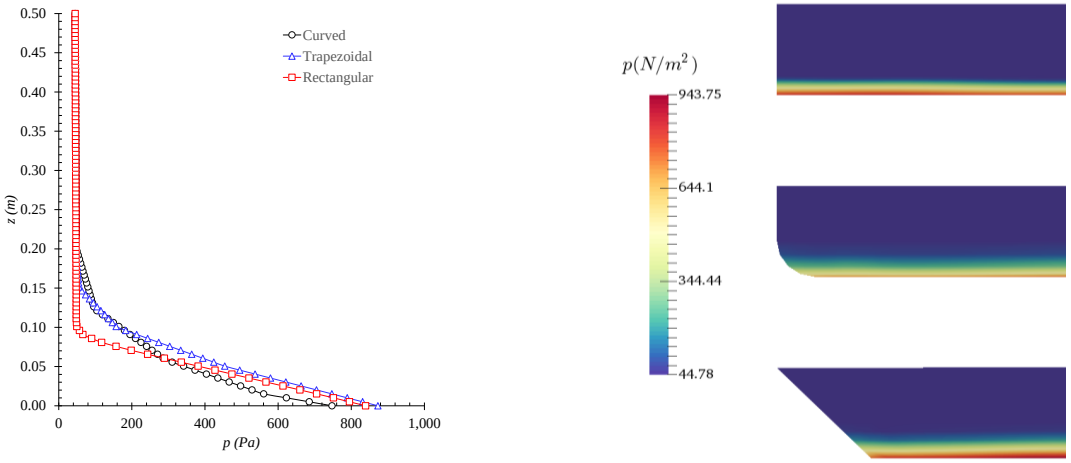

Figure 7. (Left) Pressure distribution across the depth of the domain and along the center-line of the cross sections at 10 m downstream in $t = 15\ (s)$. Pressure is calculated relative to the reference point (0, 0, 0.5) where p = 0. (Right) Corresponding pressure contours close to the side walls.

Results suggest that the early energy dissipation is more intense through curved edge rectangular cross sections compared to trapezoidal forms.

Although a curved edge rectangular cross section might have better performance at starting the energy dissipation process, pressure and velocity distributions suggest that this type of cross section is not only impractical to build but also more likely to damage the spillway slab due to uplift/stagnant pressure incidents induced by vertical offsets in bed; see Figure 7 and Figure 8.

Figure 8 shows velocity distributions at 10 and 20 m downstream. It is illustrated that the curved edge rectangular and trapezoidal cross sections causes more velocity at 10 m downstream, i.e. middle of the spillway's slab.

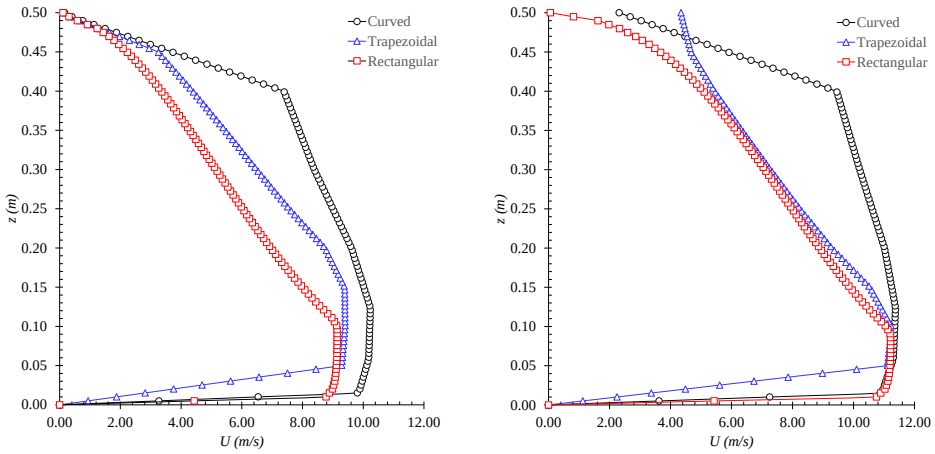

Figure 8. Stream-wise velocity profiles at 10 m (left), and 20 m (right) downstream extracted from the centerline of the cross-sections.

Hence, in cases of forward vertical offset of the bed, they may lead to higher stagnation pressure. Also, at the outlet it is shown that the three flows reach to the same maximum velocity. However, translatory waves and aeration process in trapezoidal and curved edge rectangular section can cause a varying velocity at the upper surface of the air phase. This is mainly an air-water phase interaction caused by translatory waves leading the energy dissipation.

4. CONCLUDING REMARKS

Effects of different types of cross sections on the energy dissipation procedure through smooth chute spillways are studied numerically. The multiphase flow of water and air through half a meter depth of the spillway is modeled with OpenFOAM solvers. The failure state of the Big Sandy Dam's spillway is simulated with 3.7% error in predicting the maximum stream-wise velocity and almost no error in water-air interface depth at 10 m downstream section. Horizontal velocity and phase fraction profiles across the depth of the channel suggest mixing with generated bubbles and formation of translatory waves. From the early presence of such processes in smooth spillways with trapezoidal and curved edge rectangular cross sections, it can be inferred that energy dissipation starts earlier upstream for these sections relative to the rectangular section. In addition, results imply that while these types of geometric configuration maybe of use for energy cascade purposes, they may lead to higher velocities, which delivers higher risk of stagnation or uplift pressure due to vertical offsets in the slab.

5. REFERENCES

Abbasoglu, C., and Okay, G. (1992). "The remedial structures on the spillway of Keban dam." International water power & dam construction, Wilmington Business Publishing, 44(12), 22–27.

Billington, D. P., Jackson, D. C., and Melosi, M. V. (2005). The history of large federal dams: planning, design, and construction in the era of big dams. Government Printing Office.

Bombardelli, F. A., Meireles, I., and Matos, J. (2011). "Laboratory measurements and multi-block numerical simulations of the mean flow and turbulence in the non-aerated skimming flow region of steep stepped spillways." Environmental Fluid Mechanics, Springer, 11(3), 263–288.

Chanson, H. (2015). Energy Dissipation in Hydraulic Structures. Igarss 2014, Taylor & Francis, London, UK.

Christodoulou, G. C. (1993). "Energy dissipation on stepped spillways." Journal of Hydraulic Engineering, American Society of Civil Engineers, 119(5), 644–650.

Deshpande, S. S., Anumolu, L., and Trujillo, M. F. (2012). "Evaluating the performance of the two-phase flow solver interFoam." Computational Science & Discovery, 5(1), 14016.

Ellis, J., and Pender, G. (1982). "Chute spillway design calculations." ICE Proceedings, 299–312.

Ferziger, J. H., and Peric, M. (2012). Computational methods for fluid dynamics. Springer Science & Business Media.

Hirt, C. W., and Nichols, B. D. (1981). “Volume of fluid (VOF) method for the dynamics of free boundaries.” Journal of computational physics, Elsevier, 39(1), 201–225.

Ippen, A. T., and others. (1951). “Proceedings of a Symposium on High-Velocity Flow in Open Channel.” Trans. ASCE, 116, 265–400.

Jasak, H., Tukovic, Z., and Jemcov, A. (2007). “OpenFOAM : A C ++ Library for Complex Physics Simulations ˇ.” nternational Workshop on Coupled Methods in Numerical Dynamics, Dubrovnik, Croatia, 1–20.

Jones, W. P., and Launder, Be. (1972). “The prediction of laminarization with a two-equation model of turbulence.” International journal of heat and mass transfer, Elsevier, 15(2), 301–314.

Kökp\inar, M. A., and Gö\ugü\cs, M. (2002). “High-speed jet flows over spillway aerators.” Canadian Journal of Civil Engineering, NRC Research Press, 29(6), 885–898.

Kundu, P. K., Cohen, I. M., Hu, H. H., and Publishers, E. S. (2002). Fluid mechanics. Academic Press, San Diego.

Lempérière, F., Vigny, J. P., and Deroo, L. (2012). “New methods and criteria for designing spillways could reduce risks and costs significantly.” Hydropower & Dams, (3), 120–128.

Lopes, P. (2013). “Free-surface flow interface and air-entrainment modelling using OpenFOAM.”

Montes, J. S. (1994). “Potential-flow solution to 2D transition from mild to steep slope.” Journal of Hydraulic Engineering, American Society of Civil Engineers, 120(5), 601–621.

Novák, P., Moffat, A. I. B., Nalluri, C., and Narayanan, R. (2007). Hydraulic structures. CRC Press.

Pope, S. B. (2000). Turbulent Flows. Cambridge University Press.

Reclamation, B. of. (2012). “Water Operation and Maintenance Bulletin.” Reclamation Managing Water in the west, 229.

Reinauer, R., and Hager, W. H. (1998). “Supercritical flow in chute contraction.” Journal of hydraulic Engineering, American Society of Civil Engineers, 124(1), 55–64.

Song, C. C. S., and Zhou, F. (1999). “Simulation of free surface flow over spillway.” Journal of Hydraulic Engineering, American Society of Civil Engineers, 125(9), 959–967.

Tanchev, L. (2014). Dams and appurtenant hydraulic structures. CRC Press.

Valero, D., and Bung, D. (2015). “Hybrid investigation of air transport processes in moderately sloped stepped spillway flows.” E-proceedings of the 36th IAHR World Congress, 28 June - 3 July, The Hague, the Netherlands, 1–10.